Available online at www.sciencedirect.com
ScienceDirect
Journal of Power Sources 171 (2007) 441–447
JOURNAL OF POWER SOURCES
www.elsevier.com/locate/jpowsour

Comparison of solid oxide fuel cell anode coatings prepared from different feedstock powders by atmospheric plasma spray method

Ohchul Kwon, S. Kumar, Soodong Park, Changhee Lee *

Kinetic Spray Coating Laboratory (NRL), Division of Materials Science & Engineering, Hanyang University, 17 Haengdang-dong, Seongdong-ku, Seoul 133-791, South Korea

Received 10 April 2007; received in revised form 7 May 2007; accepted 31 May 2007
Available online 19 June 2007

Abstract

Atmospheric plasma spray (APS) deposition of a high-performance anode coating, which is essential for obtaining high power density from a solid oxide fuel cell (SOFC), is developed. A conventional, micron-sized, nickel-coated graphite – yttria stabilized zirconia (YSZ) – graphite blend feedstock leads to a non-uniform layered coating microstructure due to the difference in the physical and thermo-physical properties of the components. In this research, new types of feedstock material received from a spray-drying method, which includes nano-components of NiO and YSZ (300 nm), are used. The microstructure and mechanical properties of a coating containing a nano composite that is prepared from spray-dried powders are evaluated and compared with those of a coating prepared from blended powder feedstock. The coating microstructures are characterized for uniformity, mechanical properties and electrical conductivity. The coatings prepared from spray-dried powders are better as they provide larger three-phase boundaries for hydrogen oxidation and are expected to have lower polarization losses in SOFC anode applications than those of coatings prepared from blended feedstock.

Keywords: Solid oxide fuel cell; Atmospheric plasma spraying; Nickel oxide; Yttria-stabilized zirconia; Anode coating; Ni-YSZ cermet

1. Introduction

The solid oxide fuel cell (SOFC) is a ceramic device that directly converts the chemical energies of fuel and oxidant gases into electrical energy without combustion as an intermediate step [1,2]. In general, a single fuel cell consists of two porous electrodes (anode and cathode) separated by a dense and gas-tight electrolyte. Among all the components in a SOFC, the anode plays an important role for the oxidation of fuel by which electricity is generated. To date, nickel/yttria stabilized zirconia (YSZ) cermets, in which the 8YSZ framework is a good ionic conductor and Ni dispersion is a good electronic conductor, has been used as the most common anode material for SOFC applications because of its low cost and relatively high electrocatalytic activity (low charge-transfer resistance) [3–8]. In general, the percolation threshold for the conductivity of Ni/YSZ cermets is about 30 vol.% Ni content, above which the conductivity can be increased sharply [3]. However, it is influenced by the microstructure of the anode such as the porosity, pore-size distribution and feedstock powder size, as well as the conductivity of each component. Lee et al. [8] have indicated that the Ni content should be kept below 50 vol.% with regard to the contiguity effect [8]. High porosity is necessary for the SOFC anode layer to supply fuel and remove reaction products as well as to maintain a three-phase boundary (TPB – electrolyte, electrode and gas phase), which acts as an active electrochemical site for reaction. Hence, microstructure control of the anode plays an important role in improving SOFC efficiency.

NiO/YSZ anode materials are usually prepared by mechanical mixing of commercially available NiO and YSZ powders. This method gives rise to a non-uniform distribution of the Ni phase in cermets, which leads to poor performance. Therefore, different wet chemical processes, such as sol–gel [9,10], complex formation with chelating agents [11], spray pyrolysis of a slurry YSZ in nickel acetate solution [12] and mechano-fusion

* Corresponding author. Tel.: +82 2 2220 0388; fax: +82 2 2293 4548.
E-mail addresses: nike5725@hanyang.ac.kr (O. Kwon), hai_kumars@rediffmail.com (S. Kumar), airtwenty4@hanyang.ac.kr (S. Park), chlee@hanyang.ac.kr (C. Lee).

0378-7753/$ – see front matter © 2007 Elsevier B.V. All rights reserved.
doi:10.1016/j.jpowsour.2007.05.102

process [13], have been reported. Other processes such as vapour deposition [14] and the spraying of wet powder [15] have also been examined. All these efforts are directed towards the preparation of a homogeneous nanoscale mixture of NiO and YSZ to produce a fine YSZ covered by a sub-micron NiO composite powder.

Spray-drying is a process by which a fluid feed material is transformed into a dry powder by spraying the feed into a hot medium. The feed materials are either water-based suspensions with air as the drying gas or organic solvent-based suspensions (usually ethanol) with nitrogen as the drying gas [16]. Although the microstructure of a SOFC anode can be manufactured by many methods such as tape casting, screen printing, slurry coating, PVD and so on, the thermal spray technique – especially the atmospheric plasma spray technique (APS) [17] – seems to be an economically attractive and effective method for the industrial production of SOFCs due to its merits, namely: low cost, easy operation, high deposition efficiency, and wide selection of materials [18].

The anode coating must have the following properties: phase stability in the fuel environment, adequate porosity for gas transport, a thermal expansion coefficient that matches with those of other components, and a high electrical conductivity for which more triple phase boundaries are required in the coating. In an anode-supported SOFC, the anode serves as the substrate for the whole cells and plays a most important role in the oxidation of fuel to generate electricity. To date, Ni/YSZ cermet is the most common anode material for SOFC applications because of its low cost and matching thermal expansion coefficient with other components.

In this study, a 8YSZ:Ni-coated graphite:graphite (50 vol.%: 35 vol.%:15 vol.%) blend and 8YSZ:NiO:graphite (40 vol.%: 30 vol.%:30 vol.%) spray-dried powders are thermal spray deposited on a porous metallic substrate. The oxidation, reduction and other results are reported and discussed.

2. Experiments

2.1. Feedstock characterization

Commercially available, blended feedstock powder was used and was composed of 8YSZ – 50 vol.% (8 mol% yttria stabilized zirconia, <45 μm, Sulzer Metco), Ni-coated graphite powder – 35 vol.% (mean particle size of 50 μm, Sulzer Metco), and graphite −15 vol.% (mean particle size <10 μm, Sulzer Metco).

Nickel and YSZ have a density mismatch which leads to non-uniformity in the coating layers. Hence, nickel-coated graphite is oxidized at 800 °C in air for 2 h. To co-deposit with YSZ, low density oxidized nickel-coated graphite is used instead of pure Ni powder. The densities of YSZ (5.1 g cm^{-3}) and NiO–graphite (5.8 g cm^{-3}) are very similar which leads to uniform coating properties.

The spray-dried powders used for this experiment consist of YSZ, NiO and graphite. YSZ (40 vol.%), NiO (30 vol.%) and graphite (30 vol.%) nano powders (300 nm) were ball-milled for 12 h. The nano-sized powders cannot be successfully plasma sprayed as the particles have different trajectories in the plasma flame during in-flight. To avoid this, the initial powders were reconstituted by a spray-drying method [19].

The slurry was prepared by the addition of 500 g of a mixed YSZ – NiO–graphite powder to distilled water (1 L) into which 2 g dispersant (binder) solution was added. The slurry was ball-milled with zirconia grinding media for 12 h. Then, 2 g of binder solution was added and milling was continued for another 4 h. The spray-drying process was carried out at 250 °C in a pilot spray drier. The binders used for the process were PVA

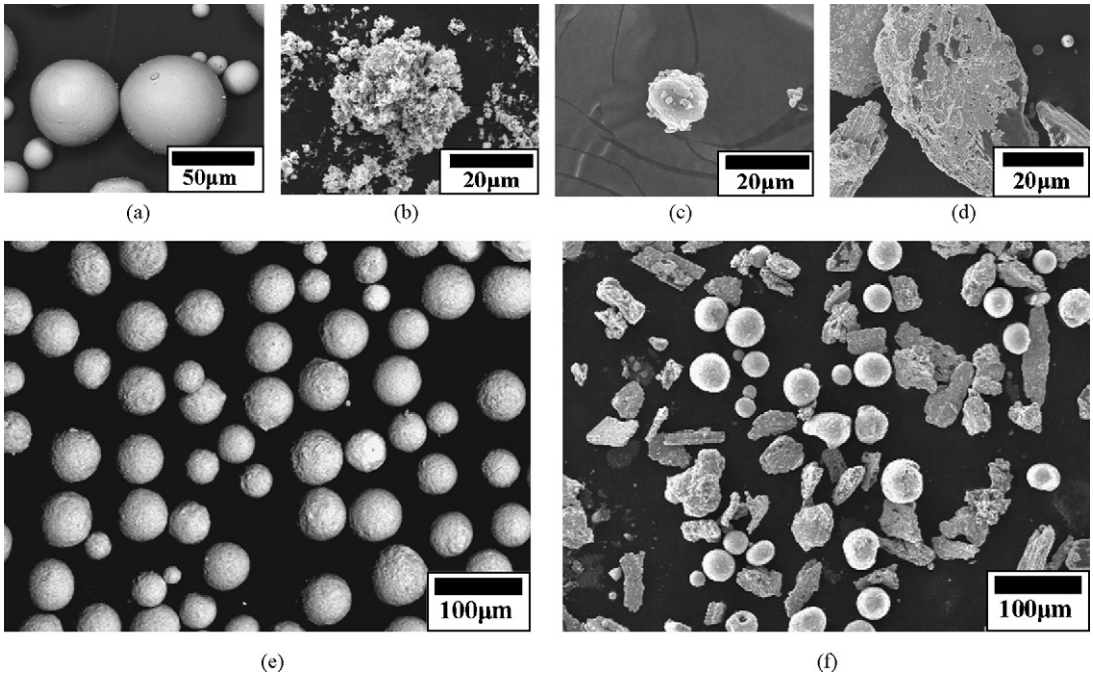

Fig. 1. Scanning electron micrographs of the feedstock materials.

(polyvinyl alcohol) MW 89,000–98,000 (1 g), PVP (polyvinyl pyrrolidone) MW 40,000 (1 g) and PEG (polyethylene glycol) MW 20,000 (0.5g). Typical process experimental parameters such as inlet temperature, outlet temperature, atomizer speed and slurry feeding rate were 240 °C, 110 °C, 8000 rpm and 3 LPH, respectively. Heat treatment of the powder was carried out in a furnace with an argon environment for good compaction between the phases.

Before spraying, characterization of the blended powder feedstock and nano-structured spray-dried powder feedstock was performed by means of scanning electron microscopy (SEM) and energy dispersion spectroscopy (EDS) analysis. Fig. 1 shows SEM images of each feedstock phases in the blended powder, namely, YSZ, NiO, graphite and nickel-coated graphite powder, respectively. It is clearly seen that the YSZ has spherical morphology, while the NiO powder is fractured. The morphologies of the graphite powder and the nickel-coated graphite are nearly spherical and irregular in shape with sharp dentric edges, respectively. Fig. 1(e) and (f) show the morphology of the spray-dried and the blended powders, respectively. The spray-dried powders are nearly uniform in size and all have spherical morphology. All the constituents of feedstock phases are clearly seen in Fig. 1(f). The size and the morphology of the powders are not uniform.

Fig. 2(a) shows the particle-size distribution of the spray-dried powder. Malvern Master Sizer particle size analyzer was used for this purpose. The size distribution ranges between 30 and 45 μm. Fig. 2(b) gives the EDX chemical mapping analysis of the spray-dried nano-composite powder. The white, grey and black parts indicate YSZ, NiO and graphite phases, respectively. The spray-dried feedstock has same chemistry and constitution ratio as that of the blended feedstock with differences in size and shape.

It is well known that the packing density of nano-sized materials to each other is higher than that of micro-sized materials due to their high surface energy and the effect of Van der Waals forces. The spray-dried powders were sintered at 1000 °C for 4 h under a flowing atmosphere of 6 vol.% H_2/N_2 to increase the cohesiveness of the powder.

2.2. Atmospheric plasma spraying

For material deposition, the method should be easy for fabrication of the coating and cost-effective. Among all other fabrication techniques, the APS procedure seems to be the most cost-effective method and a large area can be covered. One more important advantage is that APS is effective for any shape of substrate so that planar, tubular and single-chambers can be coated easily. Hence, APS has been selected. The coatings were prepared from the blended and the nano-structured spray-dried composite powder feedstocks by means of a direct current (DC) atmospheric plasma spray system (Sulzer Metco 9 MB). The APS system consists of a DC plasma torch that generates a high-temperature plasma flame under atmospheric conditions, a powder feeder for delivering plasma sprayable powders, and a cooling system for the torch. The gas used in this experiment was a mixture of argon and hydrogen. The spraying distance between the substrate and the center line of the nozzle was maintained as 100 mm. The feedstock powder was vertically injected into the plasma gas downstream at the plasma jet center line at a feed rate of 20 g min^{-1}. Also, it was injected into the plasma jet at a 45° angle to the vertical center line of the nozzle to minimize the effect of gravitational force on the powder trajectory. A porous metallic woven mesh substrate was made by spot welding, grit blasted, and cleaned by ultrasonic treatment before spraying.

In order to change the characteristics of the plasma jet, the hydrogen gas flow rate was changed while the other process parameters were held constant. The processing parameters are listed in Table 1.

Table 1
APS process parameters

Plasma gas composition		Arc current (A)	Distance (mm)	Powder feed rate (g min^{-1})
Ar (SCFH)[a]	H_2 (SCFH)[a]			
100	5/10/15	500	100	20

[a] SCFH: cubic feet per hour at standard conditions.

2.3. Characterization of coating

The microstructure and the phase composition of the coatings were observed by means of scanning electron microscopy (SEM) and energy dispersion spectroscopy (EDS). The porosity of the coatings was measured using an image analysis method. The porosity rate was calculated according to the coating cross-sectional area fraction of pores on the image by using Image Pro-Plus software. Vickers micro-hardness measurements were conducted on polished cross-sectional surfaces using a Vickers

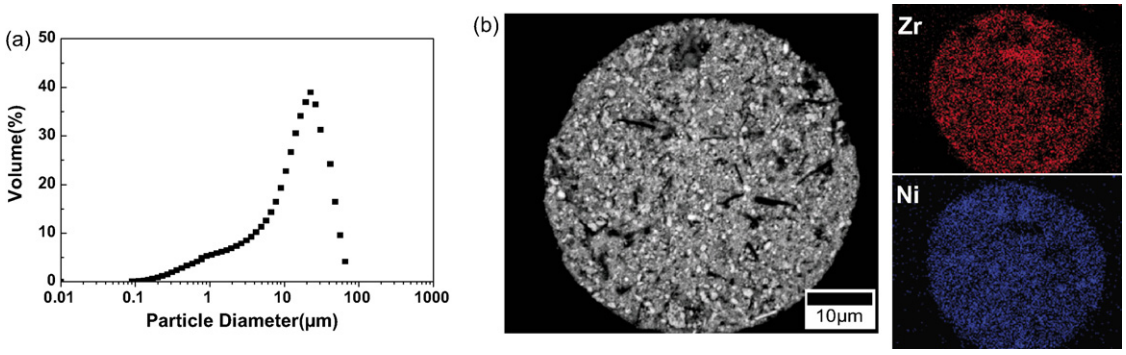

Fig. 2. Characteristics of feedstock materials.

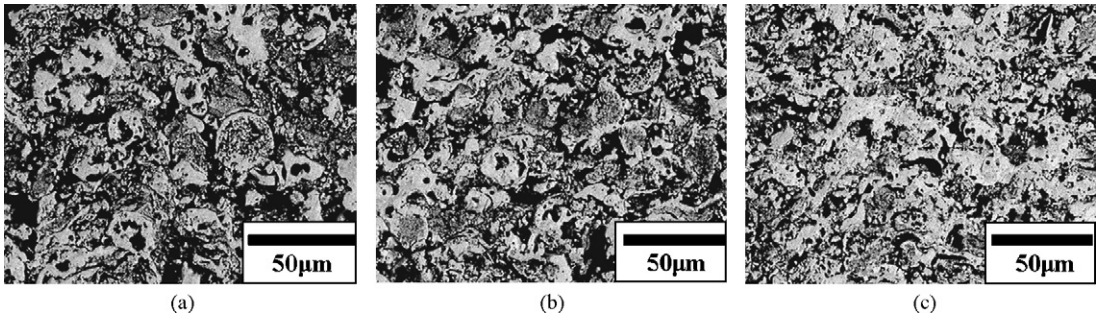

Fig. 3. Scanning electron micrographs of as-sprayed NiO/YSZ/graphite coating prepared from spray-dried powders at different hydrogen flow rates with primary gas; (a) 5 SCFH; (b) 10 SCFH: (c) 15 SCFH.

indenter with an applied load of 2.942 N. The electrical resistance was measured by a DC 4-probe method using platinum wires and a current source (Keithley 224) and multimeter (Keithley 2000) under the flow of 4 vol.% of H_2/Ar. The gas flow rate was 150 cm^3 min^{-1}. The samples were heated to 1000 °C at a heating rate of 10 °C per min and then held at this temperature for 30 min. The measurements were performed on cooling.

3. Results and discussion

3.1. Microstructure

The as-sprayed coatings were polished and characterized by SEM analysis for their microstructural analysis. The average thickness of the coating was 150 μm. Fig. 3 presents SEM images of the as-sprayed coatings prepared from NiO/YSZ/graphite spray-dried powders under different hydrogen (secondary gas) flow rates. From Fig. 3(a), it is clearly seen that some of the particles are not fully melted. In the microstructure, many unmelted and some partially-melted powders are embedded in the coating. In the microstructure, the black parts are pores. Fig. 3(b) and (c) show micrographs of the coatings prepared using 10 SCFH and 15 SCFH hydrogen flow rates, respectively (SCFH = standard cubic feet per hour). It is clearly seen that at a 10 SCFH hydrogen flow rate, all the powders are melted/partially-melted and the porosity distribution is reduced as compared with the particles shown in Fig. 3(a). At a 15 SCFH hydrogen flow rate, all the powders are melted due to the high enthalpy and the heat flux of the plasma jet. From Fig. 3(c), it is seen that all the powders are melted and a uniform coating morphology is obtained with a 15 SCFH hydrogen flow. On increasing the hydrogen flow rate, the enthalpy and the heat flux supplied to the powders are increased as hydrogen is a diatomic gas which leads to complete melting and coating formation. The porosity distribution is also uniform in the case of higher hydrogen flow rates.

Scanning electron micrographs of the as-sprayed, oxidized and hydrogen reduced coatings are shown in Fig. 4(a)–(c), respectively. The coatings were prepared from spray-dried powders. During oxidation, graphite phases present in the coating

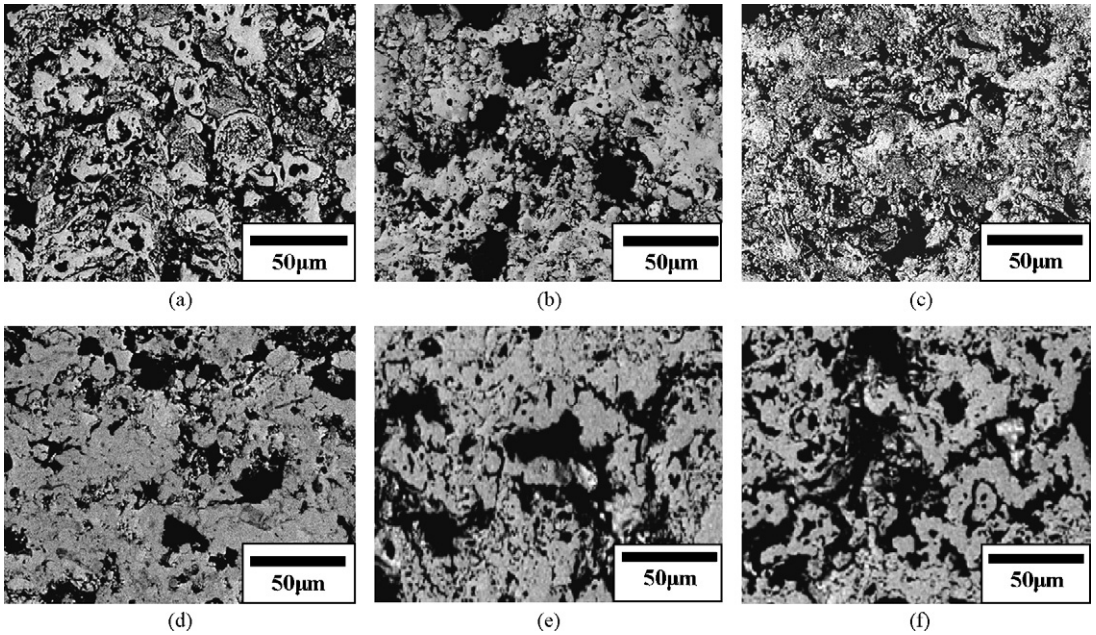

Fig. 4. Scanning electron micrographs of (a) and (d) as-sprayed, oxidized (b) and (e) and hydrogen reduced (c) and (f) coatings prepared from spray-dried and blended powders.

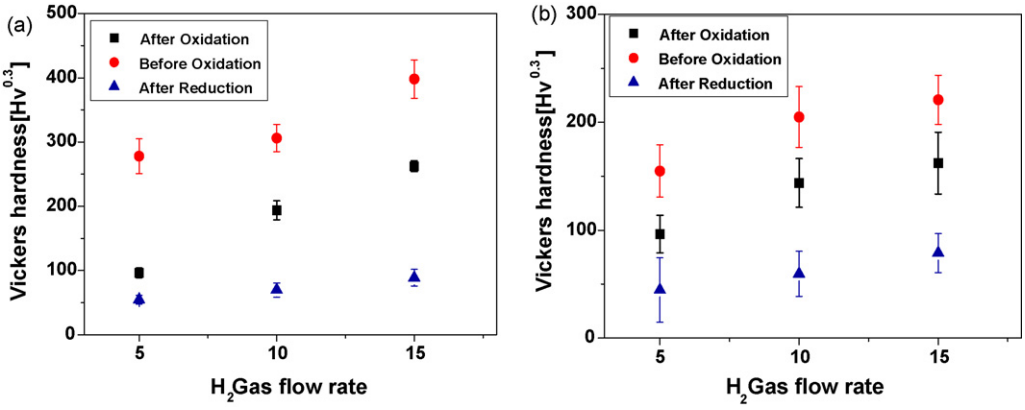

Fig. 5. Vickers hardness value of coatings (as-sprayed, after oxidation and hydrogen reduction) as function of hydrogen gas flow rate prepared from (a) spray-dried and (b) blended powders.

layer become oxidized. Hence, the porosity is increased due to the removal of graphite phases in the form of carbon dioxide. On the other hand, the distribution of pores is not uniform. This is evident from Fig. 4(b) which shows the non-uniform distribution of the graphite phase in the coating. The three-phase boundaries are formed by pores, YSZ particles and nickel on which oxidation of hydrogen occurs in a SOFC cell. The NiO particles in the coating are reduced to Ni particles and the conductivity of coating is thereby changed from that of a ceramic insulator to that of a metal conductor.

The above process also increases the porosity which enables the flow of gases in the cell. The hydrogen reduction in the coating can yield channels through which hydrogen can propagate and be oxidized with oxygen ions that come from the cathode and propagate through the YSZ electrolyte. The YSZ present in the coating forms a conductive network for negative oxygen ions while Ni forms one for electrons. During the hydrogen reduction test, the NiO phase present in the coatings is reduced and the remaining phases are YSZ and Ni. In Fig. 4(c), white and grey colours of the microstructure indicate YSZ and Ni phases, respectively. The pores are black in colour and are uniformly distributed in the coating.

A scanning electron micrograph of the coatings prepared from the blended powders is shown in Fig. 4(d). It is seen from Fig. 4(a) and (d) that the pore-size is relatively large and the distribution is not uniform for coatings prepared from the blended powders. The coatings were prepared with a 5 SCFH hydrogen flow rate. After the oxidation test of the coatings prepared from blended powder, the sizes of the pores are similar to that of coatings prepared from spray-dried powders. The relatively smaller pore distribution in the coating is comparable with coatings prepared from spray-dried feedstock which is not uniform. The distribution of pores after the hydrogen reduction test of the coatings prepared from blended powders is relatively poorer than that of the coatings prepared from spray-dried powders. This effect may lead to poor bonding of the coating with the substrate.

From the micrographs of the coatings, it is clear that the coatings prepared from spray-dried powders at higher hydrogen gas flow rate have good microstructure characteristics for applications as anodes in SOFCs.

3.2. Vickers micro hardness

Fig. 5(a) shows the Vickers hardness values of the coatings prepared from spray-dried powders. The hardness values were measured at 11 places and the average hardness was taken for analysis. For spray coatings, the value of Vickers hardness is relatively higher. It is seen from the data that the Vickers hardness value decreases for coatings after the oxidation test. During oxidation, the graphite phase present in the coating is oxidized and forms a gas-phase oxide that creates porosity. Hence, the Vickers hardness value decreases. The hardness value for coatings prepared at a 5 SCFH hydrogen flow rate is 280 kg mm^{-2}. After oxidation, for the same coating it decreases to 100 kg mm^{-2}.

The Vickers hardness measurements were taken for the same coatings after oxide reduction test in a hydrogen atmosphere. The results, shown in Fig. 5(a) show the treatment further decreases the Vickers micro hardness values. The NiO phase present in the coating becomes reduced in the hydrogen atmosphere and forms nickel which make more pores in the coating.

Increasing the hydrogen flow rate in the plasma process gas increases the micro hardness of the coatings. Hydrogen has the highest specific enthalpy and thus increases the heat flux of the plasma jet. Hence, with increasing hydrogen flow rate, more heat penetrates inside the particles and leads for better melting which reduces the porosity. This is the reason for higher Vickers hardness values at higher hydrogen flow rates. The rate of fall in the Vickers hardness for 5 SCFH hydrogen is more than that for higher hydrogen flow rates. Under 5 SCFH hydrogen flow rate conditions, particles become partially melted due to the poor heat flux present in the plasma jet. Thus, during oxidation, many unmolten/partially-molten particles may create more pores.

Fig. 5(b) gives the Vickers hardness values of coatings prepared from the blended powder. The results are the same as those for spray-dried powders. It is clear from Fig. 5(a) and (b) that coatings prepared by spray-drying have greater hardness values than those made from blended powders. For a 5 SCFH hydrogen gas flow rate, the Vickers micro hardness of the coating prepared from spray-dried powder is 280 kg mm^{-2}. For the same condi-

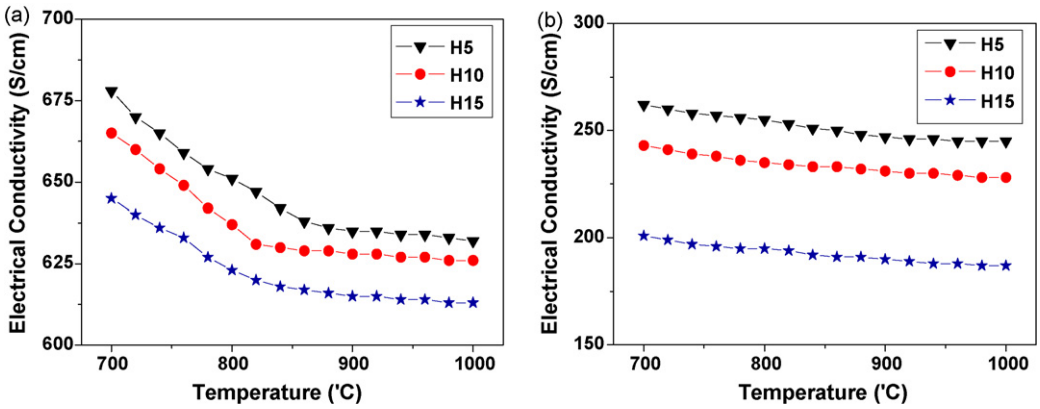

Fig. 6. Electrical conductivity of coatings prepared from (a) spray-dried and (b) blended powders at different hydrogen gas flow rates as function of operation temperature.

tions, the hardness of the coatings prepared from blended powder is 150 kg mm^{-2}. The size of the spray-dried powder is larger than that of blended powders. Thus, the heat flux transferred to the spray-dried powders is more. For blended powder, heat cannot penetrate the core/centre of the powder due to the low dwell time, higher particle size, irregular morphology, and difference in densities among phases. Also, the deviation of the measured hardness value is less in the case of spray-dried powders. This shows that the porosity distribution and the microstructure are more uniform in the coatings prepared from spray-dried powders than from blended powder.

3.3. Electrical conductivity

Fig. 6(a) and (b) presents the electrical conductivity – temperature graph for coatings prepared from spray-dried powders and blended powders, respectively. It is seen that increasing hydrogen flow rate decreases the electrical conductivity of the coatings. For coatings prepared from spray-dried powders, the effect is much higher than that of blended powder. The values are 620 and 190 S cm^{-1} at 800 °C for coatings prepared from spray-dried and blended powders, respectively. The reference anode shows the lowest electrical conductivity of 160 S cm^{-1} at 800 °C [3,8]. The rate of fall of electrical conductivity as a function of temperature is higher for coatings prepared from spray-dried powders. Nevertheless, the electrical conductivity is higher than that of blended at higher temperatures. The spray-drying of powder can provide more three-phase boundaries for the hydrogen oxidation reaction in a SOFC and is therefore expected to have a lower polarization loss for SOFC anode applications.

It is seen from Fig. 6(a) and (b) that the electrical conductivity of the coatings prepared from spray-dried powders is greater than that of blended powders. In spray-dried powders, all the phases present are very small in size and have close contact with each other. They have more three-phase boundaries in a uniform distribution. Hence, the contact between particles in the coating is very close together. In the case of blended powders, however, the phases are comparatively large and the contacts between phases are poor. This is the reason for the inferior electrical conductivity of the coatings prepared from blended powder.

4. Conclusions

Atmospheric plasma spray (APS) coatings of YSZ/Ni have been prepared from spray-dried and blended feedstock powders. The microstructure, micro-hardness and electrical conductivity of the coatings are strongly dependent on the nature of powder feedstock. Coatings prepared from spray-dried powders have nano-size phase distribution and more three-phase boundaries, which lead to higher electrical conductivity than that of the coatings prepared from blended powder due to uniform distribution of the phases throughout the coatings. A maximum electrical conductivity of 651 S cm^{-1} at 800 °C has been achieved from spray-dried powders. Even though the electrical conductivity at 800 °C of the coatings prepared by blended powder is much lower (254 S cm^{-1}) than that of spray-dried powders, the value is higher than the standard value (160 S cm^{-1}) required for electrical conductivity.

Acknowledgements

This work was supported by the Korea Science and Engineering Foundation (KOSEF) grant funded by the Korea government (MOST) (No.2006-02289).

References

[1] N.Q. Minh, T. Takahashi, Science and Technology of Ceramic Fuel Cells, Elsevier, New York, 1995, pp. 132–147.
[2] N.Q. Minh, Ceramic fuel cells, J. Am. Cerm. Soc. 76 (1993) 563–588.
[3] W.Z. Zhu, S.C. Deevi, Mater. Sci. Eng. A 362 (2003) 228–239.
[4] J. Li, Z. Lu, J. Miao, Z. Liu, G. Li, W. Su, J. Alloy. Compd. 414 (2006) 152–157.
[5] S.D. Kim, H. Moon, S.H. Hyun, J. Moon, J. Kim, H.W. Lee, Solid State Ionics 177 (2006) 931–938.
[6] H. Abe, K. Murata, T. Fukui, W.J. Moon, K. Kaneko, M. Naito, Thin Solid Films 496 (2006) 49–52.
[7] Y.L. Liu, C.G. Jiao, Solid State Ionics 176 (2005) 435–442.
[8] J.H. Lee, H. Moon, H.W. Lee, J. Kim, J.D. Kim, K.H. Yoon, Solid State Ionics 148 (2002) 15–26.
[9] V. Esposito, C. D'Ottavi, S. Ferrari, S. Licoccia, E. Traversa, Proc.—Electrochem. Soc. (2003) 643–652.
[10] M. Marinsek, K. Zupan, J. Macek, J. Power Sources 86 (2000) 383.

[11] Y. Okawa, T. Matsymoto, T. Doi, Y. Hirata, J. Mater. Res. 17 (2002) 2266.
[12] T. Fukui, S. Ohara, K. Mukai, Electrochem. Solid-State Lett. 1 (1998) 120.
[13] T. Fukui, K. Murata, S. Ohara, H. Abe, M. Naito, K. Nogi, J. Power Sources 125 (2004) 17.
[14] T. Ioroi, Y. Uchimoto, Z. Ogumi, Z. Takehara, J. Electrochem. Soc. 78 (1995) 593.
[15] N.M. Sammes, M.S. Brown, R. Ratnarai, Mater. Sci. Lett. 13 (1994) 1124.
[16] J.N. Armor, A.J. Fanelli, G.M. Marsh, P.M. Zambri, J. Am. Ceram. Soc. 71 (1988) 938–942.
[17] G. Kim, H. Choi, C. Han, S. Uhn, C. Lee, Surface Coatings Technol. 195 (2005) 107–115.
[18] R. Zheng, X.M. Zhou, S.R. Wang, T.L. Wen, C.X. Ding, J. Power Sources 140 (2005) 217–225.
[19] C. Lee, H. Choi, C. Lee, H. Kim, Surface and Coatings Technology 173 (2003) 192–200.